SOIL STRAIN RATE EFFECTS ON AXIAL PILE CAPACITY

by R. G. Bea, Ocean Engineering Division
PMB Systems Engineering, Inc.
San Francisco, California

ABSTRACT

Soil strain rate effects are known to have important influences on the load and deformation response of axially loaded piles embedded in cohesive soils. Generally, high rates of loading result in increased load resistance and stiffness. Low rates of loading result in decreased load resistance and stiffness.

In this paper, results from recent deep-penetration pile load tests (8,13) in which rapid rates of loading were applied, are used to describe strain rate effects. These results are compared with those from laboratory soil tests employing high rates of strain. A viscous damping coefficient is derived from these results.

The viscous damping coefficient is utilized in a recently developed computer code (INTRA) intended for analyses of dynamic soil-structure interactions (2). The code and damping coefficients are used in a study of the dynamic response characteristics of a pile beneath a 1000 ft water depth platform located in the Gulf of Mexico.

Based on results from an empirical approach (5), and the analytical approach discussed in this paper, substantial increases are found in the load resistance of the pile foundation subjected to typical combinations of static and dynamic loadings.

INTRODUCTION

Current (1982) offshore engineering practice is to design piles for platforms using static analyses that have been calibrated with results of static pile load tests (11,18,20).

Environmental loadings acting on platforms are dynamic, since both time varying and cyclic loadings are involved. In addition, large static loadings generally are present due to the dead weight of the structure and its operational loadings (5,25).

Recent research results from analytical models (22) and pile load tests (3,5,13) show that high rate of loading effects, derived primarily from soil strain rate effects, can substantially increase pile force resistance over that for static loadings. Cyclic loadings and sustained loadings inducing high soil strains can have offsetting effects (12,21).

Figure 1 shows a comparison of strain rate effects as indicated by pile load tests (5) and laboratory tests on soil samples (7). The pile load tests were performed on piles embedded in cohesive soils. The laboratory tests were performed on cohesive soils of moderate to high plasticity. Similar trends are noted.

A rate factor, β, which is the ratio of dynamic, P_d, to static, P_s, resistance, can be expressed as:

$$\beta = \frac{P_d}{P_s} = F_1 + F_2 \log \frac{\lambda}{\lambda_s} \quad \text{.....} \quad (1)$$

where λ_s is the reference loading rate and λ is the actual loading rate. Based on the pile load test data in Fig. 1, F_1 falls in the range of 0.75 to 1.25, and F_2 in the range of 0.10 to 0.20.

Conventional static pile load tests are performed at a rate in the range of 1 to 10 percent of ultimate capacity per hour. Extreme condition wave forces acting on a platform can produce pile head loadings in the range of 10^4 to 10^5 percent of ultimate capacity per hour. Thus, the empirical rate factor would be in the range of 1.6 to 1.8, indicating a 60 to 80 percent increase in resistance of the pile.

This paper will examine the static and dynamic axial load displacement characteristics of a typical pile in the foundation of a 1000 foot water depth, template-type platform located on the Continental Slope of the Gulf of Mexico. Soil conditions at the site consist of plastic, underconsolidated, cohesive materials.

Pile, soil and design loading conditions are utilized as input to a computer code (INTRA) intended for analyses of dynamic soil-pile-structure system interactions (2,15). Data from published pile load tests (8,13) and laboratory soil tests (4,5) are used to describe pile-soil strain rate effects in the cohesive soils. Pile response

is studied for a wide range in potential strain rate effects and combinations of static and dynamic loadings.

DEEPWATER PLATFORM FOUNDATION

Soil characteristics at the site of an example 1000 ft water depth platform in the Gulf of Mexico are given in Figs. 2, 3 and 4.

The estimated soil undrained shear strength, S_u, based on triaxial tests and the SHANSEP procedure (14) increases linearly with depth to a penetration of about 300 ft. The shear strength is then relatively constant to a depth of 500 ft.

The estimated in-situ vertical effective stress, $\bar{\sigma}_v$, based on oedometer tests is shown in Fig. 3. Comparison with the total overburden stress, σ_{vo}, indicates that these soils are generally underconsolidated. Triaxial tests indicate a $S_u/\bar{\sigma}_v$ ratio of about 0.25.

The Liquidity Index, LI, profile is shown in Fig. 4. Liquidity indices in the range of 0.8 to 1.0 at the mudline decrease to values of 0.3 to 0.4 at a penetration of 300 ft, whereupon they are relatively constant to a penetration of 500 ft.

In this example, a 72-inch diameter, open-ended steel pile having a wall thickness of 1.5 inches will be studied.

The computed axial static capacity of the pile based on API guidelines (1) and an effective stress method (10) are shown in Fig. 5. In this particular case, the two methods for computing pile capacity result in similar capacities. The pile is indicated to have a computed ultimate static capacity of 10,000 to 11,500 kips at a penetration of 400 ft.

The computed dynamic axial loading acting on the pile head for the design wave condition is shown in Fig. 6. The loading has a rise time of 2 to 3 seconds and a period of about 6 seconds. The period of the pile head axial loading is coincident with the fundamental period of the platform. The first mode is a lateral bending or flexural mode, with a large rocking component.

The peak dynamic load (compressive) is about 6400 kips. The static load on this pile due to the platform weight and drilling-production loadings is about 1800 kips. Thus, the total maximum design load is 8200 kips. Note that due to current, wind and wave drift loads, the pile does not experience tensile loadings.

If one were to use a factor-of-safety of 1.5 as suggested by API (1), then an ultimate design load of 12,300 kips would be required. This would require a pile penetration of 450 to 500 feet for an equivalent static capacity.

If, based on the data in Fig. 1, one were to rationalize that the dynamic component of the design load could increase the effective resistance of the pile by a factor of 1.4 to 1.8, then an equivalent

static load of 3600 to 4600 kips could be computed (6400 kips/1.4 to 1.8). Adding this equivalent static load to the static load would give an equivalent total static design load of 5400 to 6400 kips. Again, using a factor of safety of 1.5 would give a design ultimate load of 8100 to 9600 kips. Pile penetrations between 350 and 380 ft would be required.

For the purpose of this example, a pile penetration of 400 ft will be assumed. In lieu ofthe foregoing empirical approach, an analytical approach based on more fundamental principles will be used to investigate the response of the pile to static and dynamic loadings.

DYNAMIC MODEL

The computer code INTRA (2,5,15) was developed to analyze the nonlinear response of pile-supported offshore platforms subjected to static and dynamic loads. It is an efficient, design-oriented code capable of performing time-domain analyses of platform system response to three-dimensional loadings or motions.

The code utilizes a finite element idealization of the structure, piles and surrounding soils. The finite elements are capable of modeling the non-linear, hysteretic behavior of structural, pile and soil elements. Other sources of damping are modeled with viscous dampers.

In this study, the pile-soil system was modeled as shown in Fig. 7. The pile was modeled with INTRA linear truss elements (15) rather than nonlinear truss elements, since elastic response of the pile itself was expected.

Spacing between the pile nodes was chosen to develop a structural discretization whose dynamic response satisfactorily approximated the continuous system. Wave equation analyses indicated that node spacing should not exceed 8 to 10 pile diameters (48 to 60 ft).

The masses shown include the weight of the pile and the weight of the soil inside the pile (pile assumed fully filled).

Soil response along the sides of the pile and at its tip are modeled with elasto-plastic, non-softening hysteretic elements. In this study, compressive and tensile branches of the force-displacement characterizations were assumed to be the same.

The values of maximum static soil resistance along the pile are tabulated in Fig. 7. The relative deformation between pile and soil at yield was assumed to be 0.2 inches along the pile shaft (8) and as 10 percent of the pile diameter at its tip (26).

INTRA models radiation or geometric damping and strain rate dependent components of soil behavior with viscous dampers. The velocity dependent force, F_D, is

$$F_D = C \dot{x} \quad \text{.....} \quad (2)$$

where C is a damping coefficient and $\dot{x}$ is the relative velocity between the pile and soil element.

Radiation damping is due to propagation of energy away from the vibrating pile. This source of energy dissipation is dependent on pile-soil stiffness, frequency and mode of loading and pile material and geometry (length, radius) (19,23).

For this problem, insight into the potential magnitude of this source of energy loss can be gained by examining the magnitude of the dimensionless frequency factor, a_o:

$$a_o = \frac{\omega r}{V_s} \quad \text{.....} \quad (3)$$

where r is the pile radius, ω is the circular frequency of the loading, and V_s is the shear wave velocity of the soil (19,23).

For a pile radius of 3 ft, a loading period of 6 seconds and a soil shear wave velocity in the range of 500 to 1000 ft/sec, a_o is in the range of 0.003 to 0.006. For this range, radiation damping effects are indicated to be negligible (19,23).

The combined static and soil strain rate resistance, F, can be expressed as

$$F = Kx + C\dot{x} \quad \text{.....} \quad (4)$$

where K is the elastic stiffness of the soil-pile element and x is the relative displacement between the pile and soil element. Thus,

$$F = F_s + C\dot{x} \quad \text{.....} \quad (5)$$

Now, letting

$$C = J' F_s \quad \text{.....} \quad (6)$$

Then

$$F = F_s + J' F_s \dot{x} \quad \text{.....} \quad (7)$$

Solving for the damping parameter J',

$$J' = \frac{\left(\frac{F}{F_s} - 1\right)}{\dot{x}} = \frac{\beta - 1}{\dot{x}} \quad \text{.....} \quad (8)$$

The damping parameter is the same as that used in wave equation analyses of pile driving (16,24).

Note in Eqn. 8 that, given the static resistance, total static and dynamic resistance, and the velocity of loading producing the total resistance, one can determine the rate parameter, J'. The corresponding damping coefficient can then be determined from Eqn. 6.

STRAIN RATE CHARACTERIZATION

Three sources of data on strain rate effects were used; pile load tests, laboratory soil tests, and laboratory rod-shear tests. Each of these sources are discussed in the following paragraphs.

Pile Load Tests. Results from an extensive series of static and dynamic pile load tests performed in Gulf Coast plastic clays have been published (8,13). These tests were performed on four short segments of 14-inch diameter steel piles driven to penetrations of 115 to 360 ft.

Load-displacement and load-displacement-time characteristics for one of these pile segments is shown in Figs. 8 and 9. Displacements are those of the test pile segment at the top of the soil interval tested.

Comparison of static and dynamic ultimate capacities in Fig. 8 indicate an increase in resistance of 80 to 90 percent (β = 1.8 to 1.9). The rate of loading was 3 to 3.5 times that used for the static tests. Examination of the published data (13) indicates that the initial static capacity loadings were developed in periods of 4 to 10 days. Thus, static loading rates, expressed as percent of ultimate capacity per hour (3), of 1 to 0.5 percent per hour were used.

Other tests in the series indicate β's in the range of 1.4 to 1.7 for loading rates 3 to 3.5 times that for the static tests. Kraft, et al (13) note that triaxial tests on the soils from this site indicated β's in the range of 1.5 for 3 orders of magnitude change in strain rate comparable to that determined in the pile tests.

Using the load test data in Figs. 8 and 9, one can derive a rate parameter and damping coefficient with P_S = 340 kips, and P_D = 625 kips. Thus,

$$\beta = \frac{P_D}{P_S} = 1.8 \quad \text{.....} \quad (9)$$

From Fig. 9:

$$\dot{x} = \frac{1.1 \text{ in}}{7 \text{ sec}} = 0.16 \text{ in/sec} \quad \text{.....} \quad (10)$$

Thus,

$$J' = \frac{1.8 - 1.0}{0.16 \text{ in/sec}} = 5.24 \frac{\text{sec}}{\text{in}} = 62 \frac{\text{sec}}{\text{ft}} \quad \text{.....} \quad (11)$$

or

$$C = J'P_s = 62(P_s) \frac{\text{kip-s}}{\text{ft}} \quad \ldots\ldots\ldots\ldots\ldots\ldots \quad (12)$$

For $\beta = 1.4$, $J' = 31$ sec/ft.

Laboratory Soil Tests. Figure 10 shows the increase in soil shear strength per log cycle increase in strain rate, ΔS_u, versus the soil Liquidity Index. These results were developed from triaxial tests performed on clays from the Gulf of Mexico and other similar locations (6,9,27). The samples were tested at an overconsolidation ratio, OCR, of 1.0. Other samples tested at higher OCR's developed trends parallel to the one shown in Fig. 10, with the ordinates multiplied by the OCR (5).

These results can be expressed in the same form as Eqn. 1, with $F_1 = 1.0$ and,

$$F_2 = \frac{OCR}{S_u/\bar{\sigma}_v} \exp \frac{LI-2}{0.42} \quad \ldots\ldots\ldots\ldots\ldots\ldots\ldots \quad (13)$$

For the soils at the example platform site (OCR = 1.0), $S_u/\bar{\sigma}_v = 0.25$, and in the lower third of the pile, $LI \cong 0.35$. Thus,

$$\beta = 1.0 + \frac{1.0}{0.25} \exp \frac{0.35-2}{0.42} \log \frac{\lambda}{\lambda_s} \quad \ldots\ldots\ldots\ldots \quad (14)$$

$$\beta = 1 + 0.07 \log \frac{\lambda}{\lambda_s} \quad \ldots\ldots\ldots\ldots\ldots\ldots\ldots \quad (15)$$

for a 3 to 4 order of magnitude increase in strain rate, $\beta = 1.3$ to 1.4.

These results indicate rate parameters in the lower range of that determined from the pile load tests.

Rod Shear Tests. Rod shear tests are laboratory tests in which a steel rod is passed through the center of a soil specimen confined inside a triaxial cell (4). After consolidation of the sample, the rod is loaded and the soil-steel interface strength determined.

Two series of rod shear tests were performed on a normally consolidated silty clay from the Gulf of Mexico (4). The first series was performed at a loading rate of 0.05 inches per minute, and the second at 0.40 inches per minute. The higher strain rate produced interface shear strengths that were approximately 30 percent greater than those at the lower rate.

These results imply about a 30 percent increase in strength for each order of magnitude increase in strain rate. This would produce a β of about 1.9 for 3 orders of magnitude increase in strain or loading rate, at the upper bound indicated by the pile load tests.

ANALYTICAL RESULTS

Based on the foregoing results, the INTRA pile-soil model was supplied with soils rate factors, J', of 0 sec/ft, 31 sec/ft, and 62 sec/ft.

The viscous damping coefficients were then determined from the static soil resistance for a given pile-soil element (Fig. 7) using Eqn. 6. This allowed an analytical description of the soil strain rate effect that would vary continuously with time, depending on the computed relative velocity between the pile-soil elements. To simulate energy losses in the pile itself, a damping ratio of 2 percent of critical was added to the soil damping coefficients.

To investigate response of the pile to the design loadings, multiple cycles of the load time history in Fig. 6 were applied at the head of the pile. The design static load of 1800 kips was simultaneously applied at the pile top.

The computed pile tip and bottom displacement-time histories during the fifth cycle of loading are shown in Fig. 11. This case is for a J' = 0, or no strain rate dependent resistance.

The static displacement at the pile head is about 0.04 ft. The peak static plus dynamic displacement at the pile head and tip are about 0.26 ft. and 0.015 ft, respectively. At the design loading, the pile displacements are within acceptable limits.

To investigate response of the pile to ultimate state static and dynamic loadings, a constant value static load of 1800 kips was applied at the pile head. Then the ordinates of the load time history in Fig. 6 were uniformly scaled up to produce the maximum total (static and dynamic) loadings indicated in Fig. 12. The displacements of the pile tip were then determined using the INTRA model.

Figure 12 shows the maximum displacements at the pile tip at the end of the fifth cycle of loading for various magnitudes of maximum pile top loading. The static load-displacement response is shown as reference to two computed dynamic load-displacement responses, one for J' = 31 sec/ft and one for J' = 62 sec/ft.

The results in Fig. 12 indicate that the soil strain rate and dynamic loading effects are producing an effective ultimate resistance that is 12,500 to 15,000 kips as compared to 10,500 kips static resistance (β= 1.2 to 1.4).

Applying a factor-of-safety of 1.5 to the total static and dynamic design load of 8,200 kips results in an ultimate design load of 12,300 kips. The 400 ft penetration pile is indicated to be satisfactory from a load resistance standpoint, even though the static capacity is only 10,500 kips.

The concern now shifts to the permanent displacements developed in the pile during extreme loadings. To investigate this behavior, the

cumulative permanent displacements at the pile tip were analyzed as a function of the magnitude and cycles of dynamic loading.

In this study, the ordinates of the design load-time curve in Fig. 6 were increased by factors of 1.5 and 2.0. The gravity load of 1800 kips was held constant. The load-time curves were repeated for a large number of cycles. It is to be noted that it is not reasonable to expect a large number of cycles of these extreme ultimate state loadings; the results generated give a picture of expected response at the ultimate or limit state.

Figure 13 summarizes the results. The maximum cumulative displacements at the pile tip are plotted against the number of cycles of applied dynamic loadings. Results are shown for the design load, 1.5 and 2.0 times the design load, and a soil rate parameter of J' = 62 sec/ft.

The results indicate maximum cumulative permanent displacements at the pile tip of less than 0.03 ft for a dynamic load factor of 1.5 for up to 10 cycles of loading. Much larger displacements are shown at a dynamic load factor of 2.0.

Satisfactory performance of the 400 ft penetration pile is indicated for dynamic load factors less than 1.5 times the design load, even though the static ultimate capacity is only about 1.25 times the design load.

It is important to remind the reader that the resistance reducing effects of cyclic loadings have not been taken into explicit account in the analyses. Pile load tests (5,12,13), model tests (17), and laboratory rod shear tests (4) indicate that as long as one is concerned with a small number of one-way cyclic loadings in which the applied loadings or displacements are less than 70 to 80 percent of the static yield load or displacements, cyclic deterioration will be small.

These observations applied to this example indicate that the 400 ft penetration pile can be expected to perform satisfactorily, i.e., the permanent displacement of the pile can be expected to be within acceptable limits with a sufficient factor-of-safety.

CONCLUSIONS

The principal conclusion from this study is that soil strain rate effects are important to the response of deep penetration, high capacity offshore piles subjected to dynamic loadings and embedded in cohesive soils. An analytical and design method, based on pile load tests and laboratory tests, has been presented to account for such effects.

For a realistic example of a pile supporting a 1000 ft water depth platform in the Gulf of Mexico, increases in load resistance of 20 to 40 percent were found for design static and wave induced dynamic loadings. Permanent displacements were found to be within acceptable limits for design loadings. Factors-of-safety between design and ul-

timate state resistances on loadings and displacements were found to be acceptable.

In terms of pile penetration, recognition of strain rate effects for dynamic wave loadings indicates a pile penetration of about 400 ft compared to a penetration of 450 to 500 ft based on static methods. Due to the high costs associated with driving such piles offshore, significant cost savings are implied if the design is based on recognition of strain rate effects.

Much work remains to be done before this approach can be commended to everyday design use. Additional pile load tests and laboratory tests are needed.

ACKNOWLEDGMENTS

This paper is a compilation of results from a large number of studies of the response of foundations supporting deepwater platforms. The author would like to recognize the contributions of Jean M. E. Audibert (Ertec), and Partha Sircar (Law Engineering), who collaborated on the work. The assistance of David Engle (Union Oil Co.), Grant Thompson (Mobil Research & Development), Ben Murphy (Amoco) and Pete Arnold and John Ruser (Shell Oil Co.) in the work and review of this paper is acknowledged.

Woodward-Clyde Consultants and PMB Systems Engineering provided the support to prepare this paper. This support is gratefully acknowledged.

REFERENCES

1. American Petroleum Institute (1979), "Recommended Practice for Planning, Designing and Constructing Fixed Offshore Platforms," API RP 2A, Section 2, Foundation Design, 10th Ed., New York, N.Y., March.

2. Arnold, P., et al., "A Study of Soil-Pile-Structure Systems in Severe Earthquakes," Proceedings, Ninth Annual Offshore Technology Conference, Houston, TX., Vol. 1, Paper OTC 2749, May, 1977, pp. 189-202.

3. Audibert, J. M. E. and Dover, A. R., (1981), Discussion of "Pile Load Tests: Cyclic Loads and Varying Load Rates" by Leland M. Kraft, Jr., William R. Cox, and Edward A. Verner (ASCE Proc. Paper 16000).

4. Bea, R. G. and Doyle, E. H., "Parameters Affecting Axial Capacity of Piles in Clay," Proceedings, Seventh Annual Offshore Technology Conference, Houston, Tx., Vol. 2, Paper OTC 2307, May, 1975, pp. 611-623.

5. Bea, R. G., "Dynamic Response of Piles in Offshore Platforms,"Proceedings, Geotechnical Engineering Division, ASCE National Convention, October 30, 1980, pp. 80-109.

6. Bjerrum, L., Simons, N. and Torbiaa, I., "The Effect of Time on the Shear Strength of a Soft Marine Clay," Proceedings, Brussels Conference on Earth Pressure Problems, Vol. 1, 1958, pp. 148-158.

7. Casagrande, A. and Wilson, S. D., "Effect of Rate of Loading on the Strength of Clays and Shales at Constant Water Content," Geotechnique, June 1951.

8. Cox, W. R., Kraft, L. M., and Verner, E. A., "Axial Load Tests on 14-Inch Pipe Piles in Clay," Proceedings, Eleventh Annual Offshore Technology Conference, Houston, Tx., Vol. 2, Paper No. OTC 3491, May, 1979, pp. 1147-1158.

9. Crawford, C. B., "The Influence of Rate of Strain on Effective Stresses in Sensitive Clay," ASTM STP 254, Symposium on Time Rates of Loading in Soil Testing, Papers on Soils, 1959, pp. 36-48.

10. Esrig, M. I. and Kirby, R. C., "Soil Capacity for Supporting Deep Foundation Members in Clay," Behavior of Deep Foundations, Raymond Lundgren, Ed., American Society for Testing and Materials, Special Technical Publication 670, June, 1979, pp. 27-63.

11. Focht, J.A., Jr. and Kraft, L. M., Jr., "Progress in Marine Geotechnical Engineering," Journal of the Geotechnical Engineering Division, ASCE, Vol. 103, No. GT10, Oct. 1977, pp. 1097-1118.

12. Grosch, J. J. and Reese, L. C., "Field Tests of Small-Scale Pile Segments in a Soft Clay Deposit Under Repeated Axial Loading," Proceedings, Twelfth Annual Offshore Technology Conference, Houston, Tx., Vol. 4, Paper No. OTC 3869, May 1980, pp. 143-151.

13. Kraft, L. M., Cox, W. R., and Verner, E. A., "Pile Load Tests: Cyclic Loads and Varying Load Rates," Journal of the Geotechnical Engineering Division, ASCE, Vol. 107, No. GT1, January 1981.

14. Ladd, C. C., et al., "Stress-Deformation and Strength Characteristics," State of the Art Report, Proceedings, Ninth International Conference on Soil Mechanics and Foundation Engineering, Tokyo, Vol. 2, 1977, pp. 421-494.

15. Litton, R. W., et al., "Efficient Numerical Procedures for Nonlinear Seismic Response Analysis of Braced Tubular Structures," presented at Oct. 17-21, 1977 ASCE Annual Convention on Inelastic Behavior of Members and Structures, held at San Francisco, Calif., (Preprint 3302).

16. Lowery, L. L., et al., "Pile Driving Analysis - State-of-the-Art," Research Report 33-13 (Final), Texas Transportation Institute, Texas A&M Univ., Jan. 1969.

17. Matlock, H. and Holmquist, D. V., "A Model Study of Axially Loaded Piles in Soft Clay," report to the American Petroleum Institute, March, 1976.

18. McClelland, B., "Design of Deep Penetration Piles for Ocean Structures," Journal of the Geotechnical Engineering Division, ASCE, Vol. 100, No. GT7, July, 1974, pp. 705-747.

19. Novak, M. and Aboul-Ella, F., "Stiffness and Damping of Piles in Layered Media," Proceedings, Earthquake Engineering and Soil Dynamics, ASCE Geotechnical Engineering Division Specialty Conference held at San Francisco, Calif., Vol. 2, June, 1978, pp. 705-719.

20. Olson, R. E. and Winter, D. G., "Review and Compilation of Pile Test Results, Axial Pile Capacity," Final Report submitted to the American Petroleum Institute, Geotechnical Engineering Report GR-81-14, Dept. of Civil Engineering, University of Texas, Austin, TX, April 15, 1981.

21. Puech, A. and Jezequel, J-F., "The Effects of Long Time Cyclic Loadings on the Behavior of a Tension Pile", Proceedings, 12th Annual Offshore Technology Conference, Houston, Tx., Paper No. OTC 3870, May 1980.

22. Poulos, H. G., "Cyclic Axial Response of Single Pile," Journal of the Geotechnical Engineering Division, ASCE, Vol. 107, No. GT1, January 1981.

23. Roesset, J. M., "Stiffness and Damping Coefficients of Foundations," Proceedings, Geotechnical Engineering Division, ASCE National Convention, October 30, 1980.

24. Smith, E. A. L., "Pile Driving Analysis by the Wave Equation," Journal of the Soil Mechanics and Foundations Division, ASCE Vol. 86, No. SM4, Proc. Paper 2574, Aug. 1960, pp. 35-61.

25. Sterling, G. H., Cox, B. E. and Warrington, R. M., "Design of the Cognac Platform for 1025 Feet Water Depth, Gulf of Mexico," Proceedings, Eleventh Annual Offshore Technology Conference, Houston, Tx., Vol. 2, Paper No. OTC 3494, May 1979, pp. 1185-1198.

26. Vesic, A. S., "Design of Pile Foundations, "Research Report to Transportation Research Board, National Research Council, Washington, D.C., 1977, 68 pp.

27. Whitman, R. V., "The Response of Soils to Dynamic Loadings," Report 26: Final Report, U. S. Army Engineer Waterways Experiment Station, May 1970.

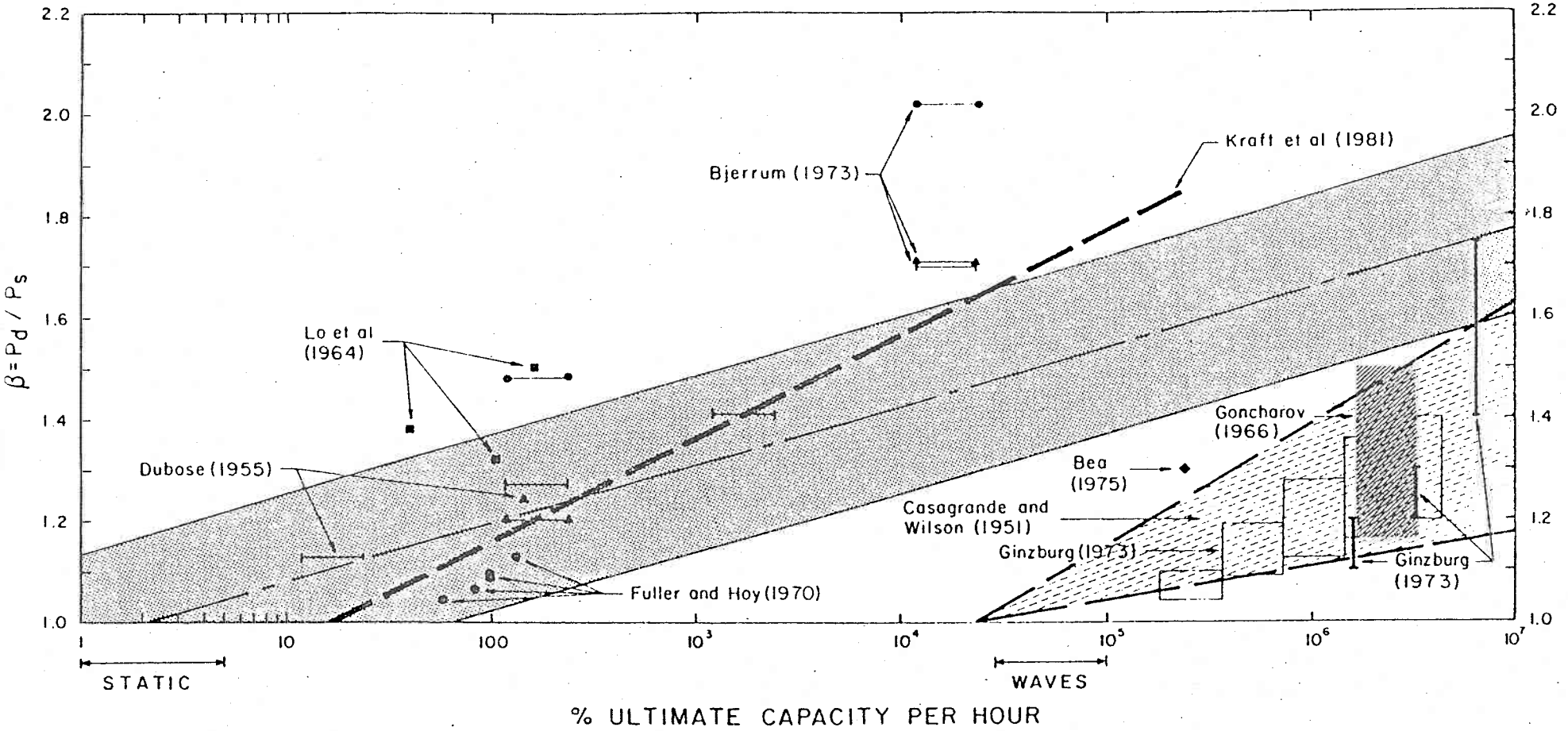

FIG. 1 RATE OF LOADING EFFECT BASED ON PILE LOAD TESTS AND LABORATORY SOIL TESTS

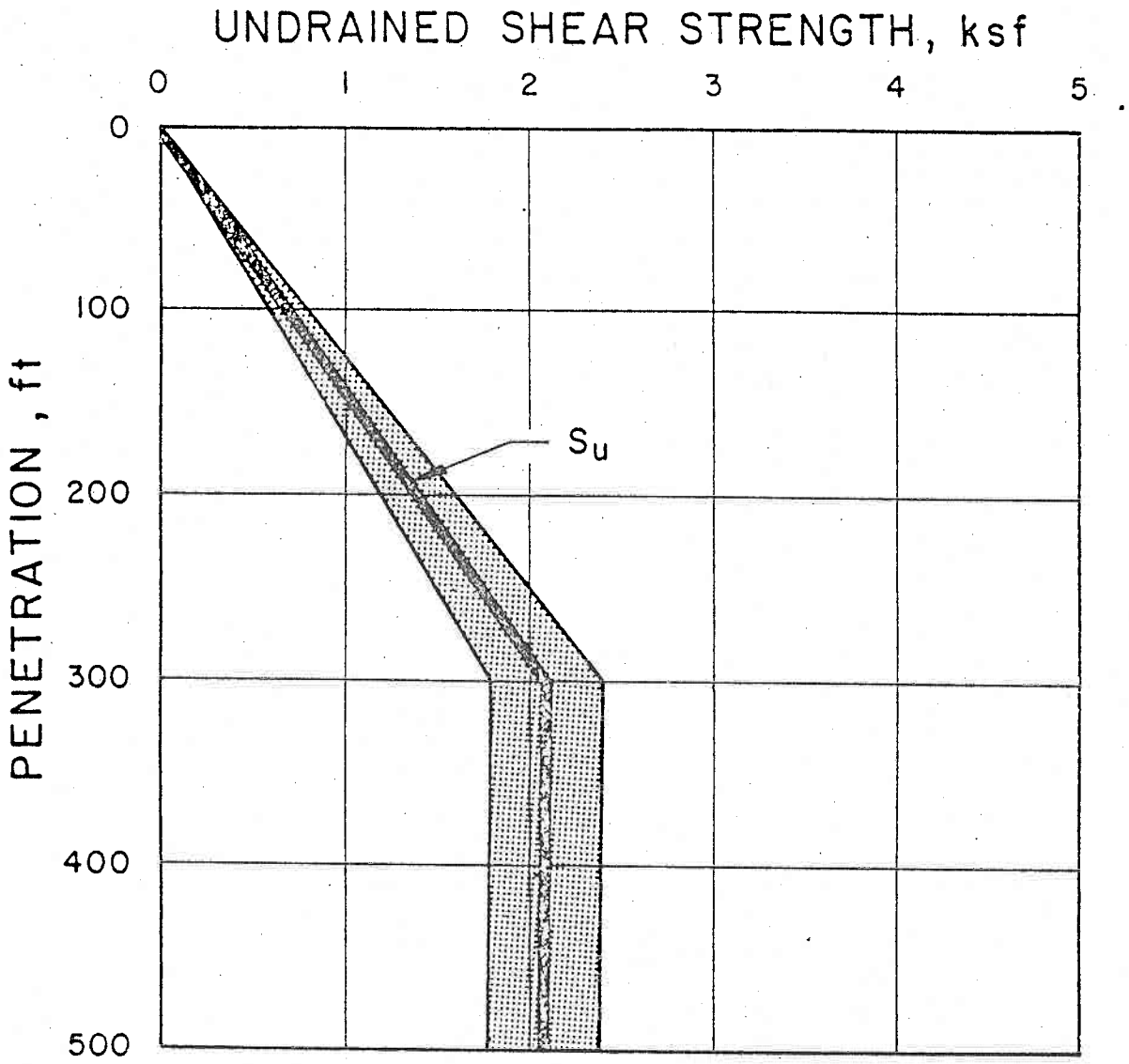

FIG. 2 SOIL SHEAR STRENGTH AT EXAMPLE PLATFORM SITE IN 1000 FEET OF WATER, GULF OF MEXICO

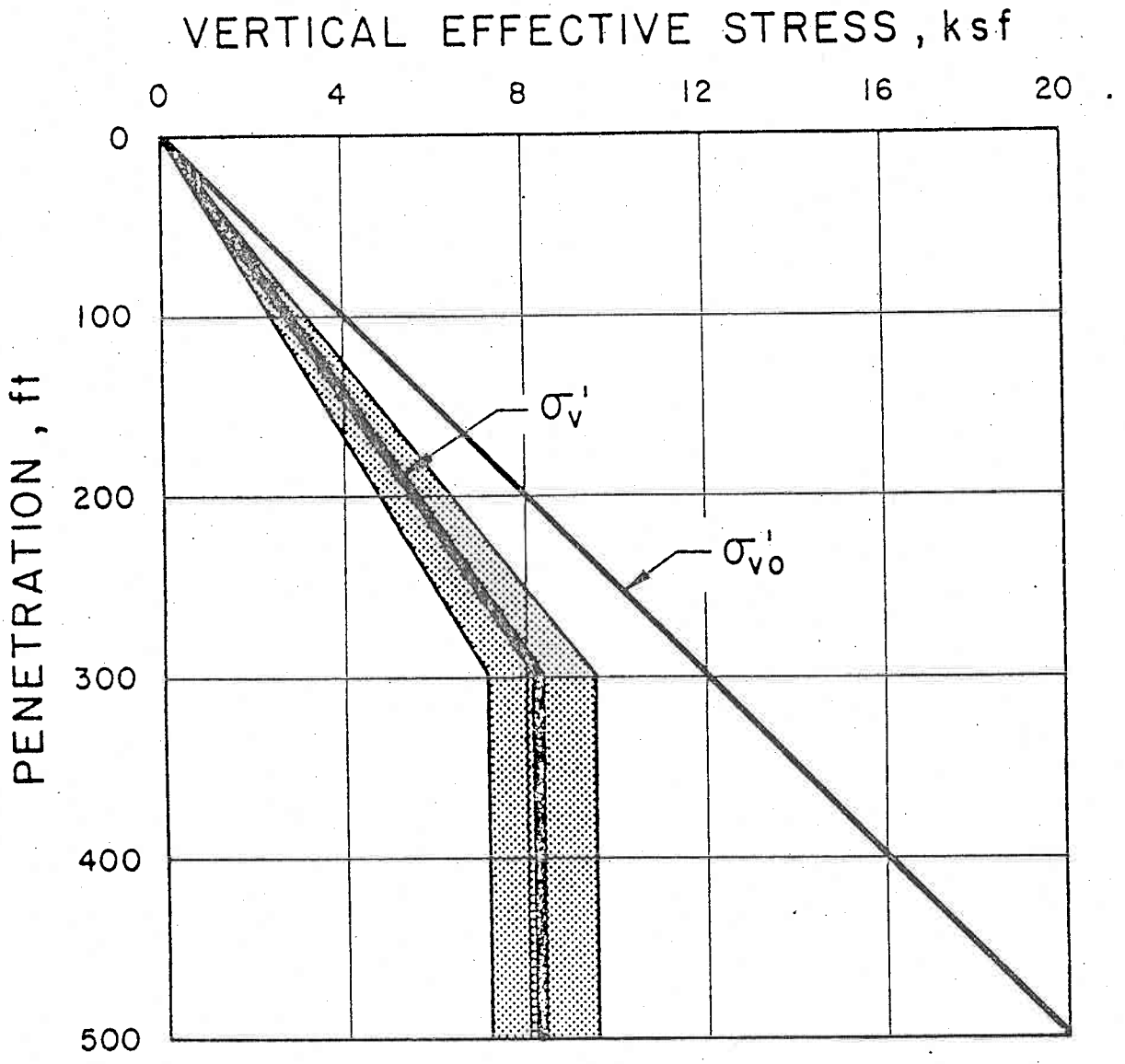

FIG. 3 VERTICAL EFFECTIVE STRESSES AT EXAMPLE PLATFORM SITE

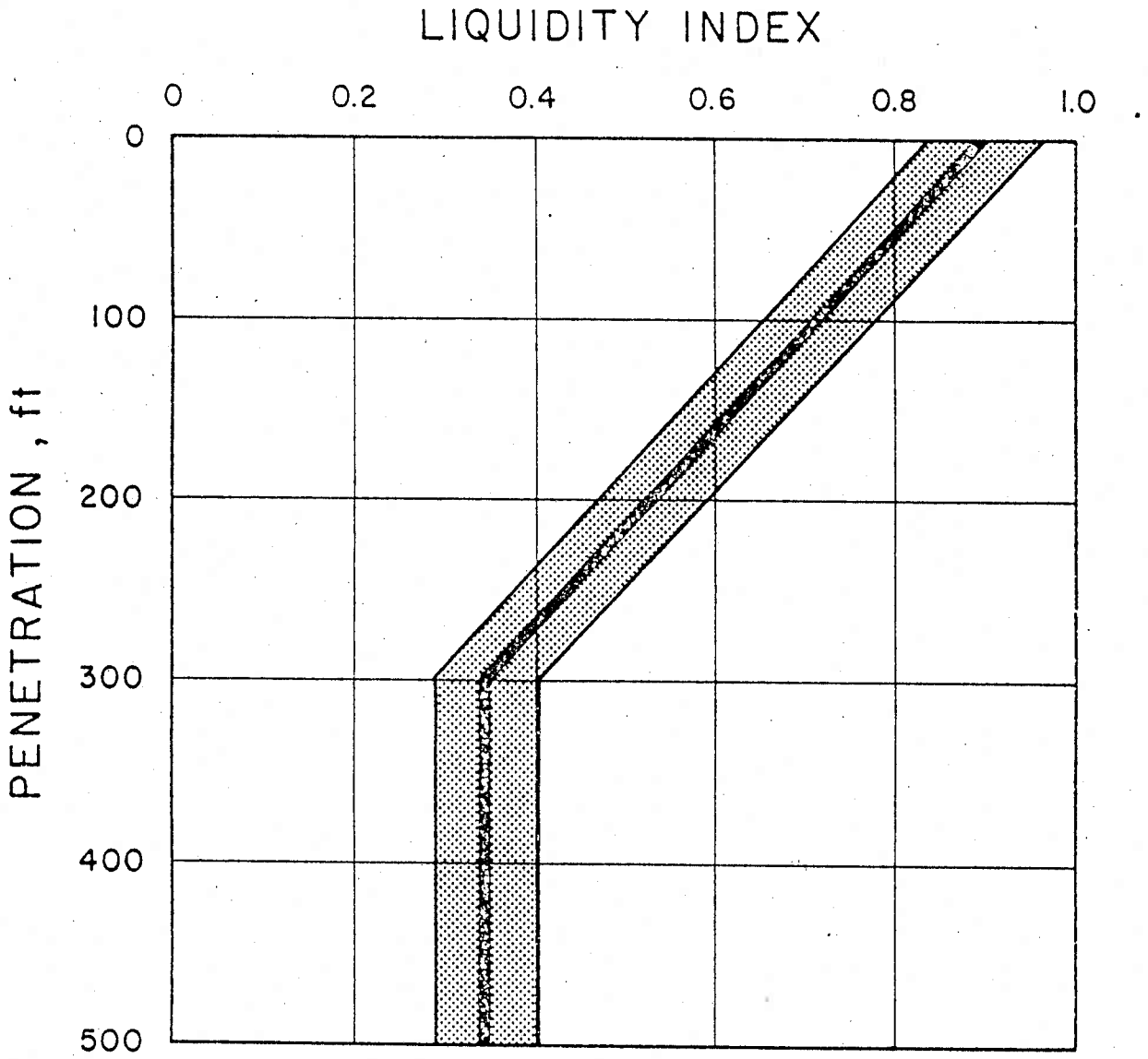

FIG. 4 SOIL LIQUIDITY INDICES AT EXAMPLE PLATFORM SITE

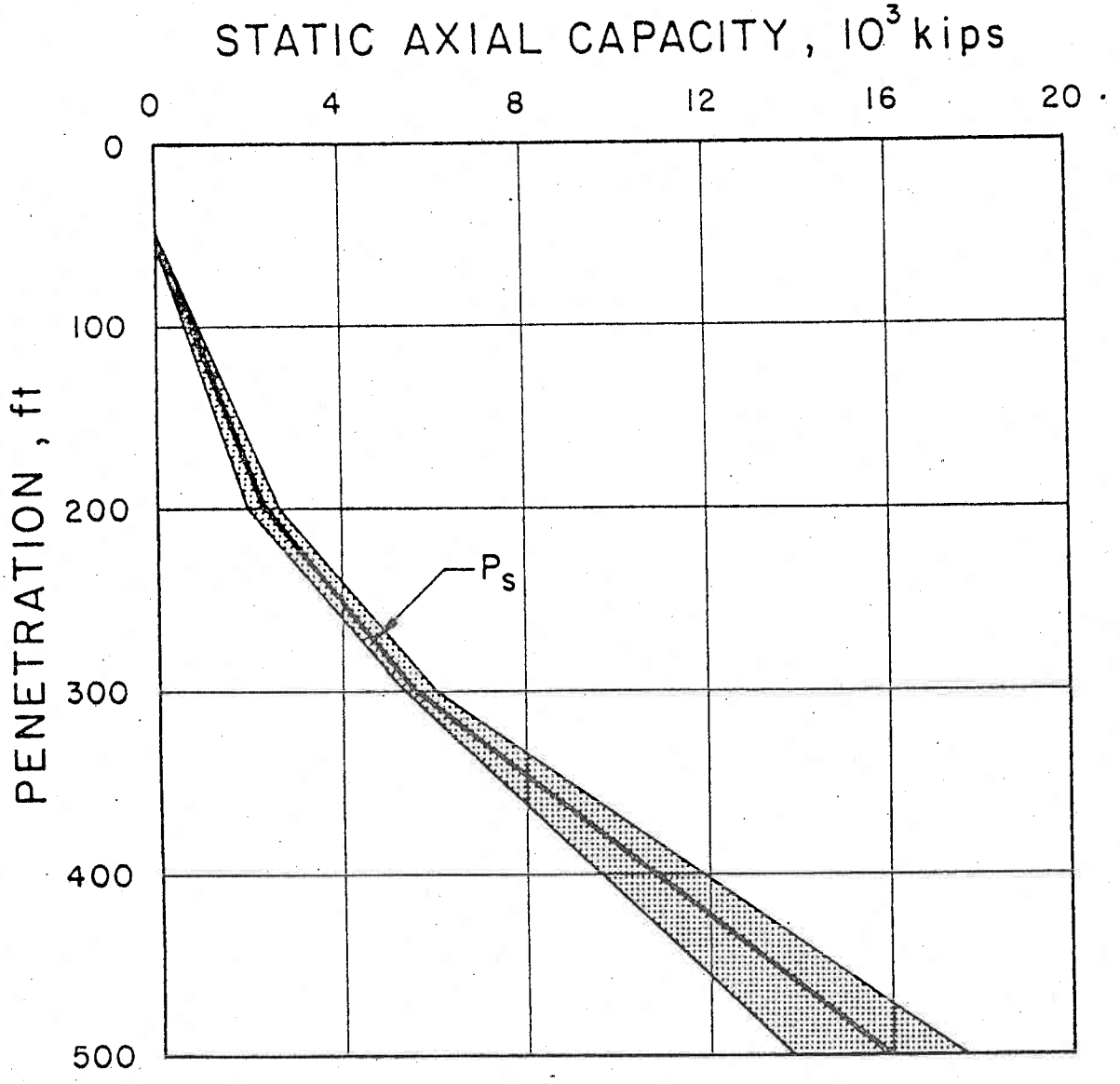

FIG. 5 COMPUTED STATIC AXIAL CAPACITY OF 72-INCH DIAMETER PILE AT EXAMPLE PLATFORM SITE

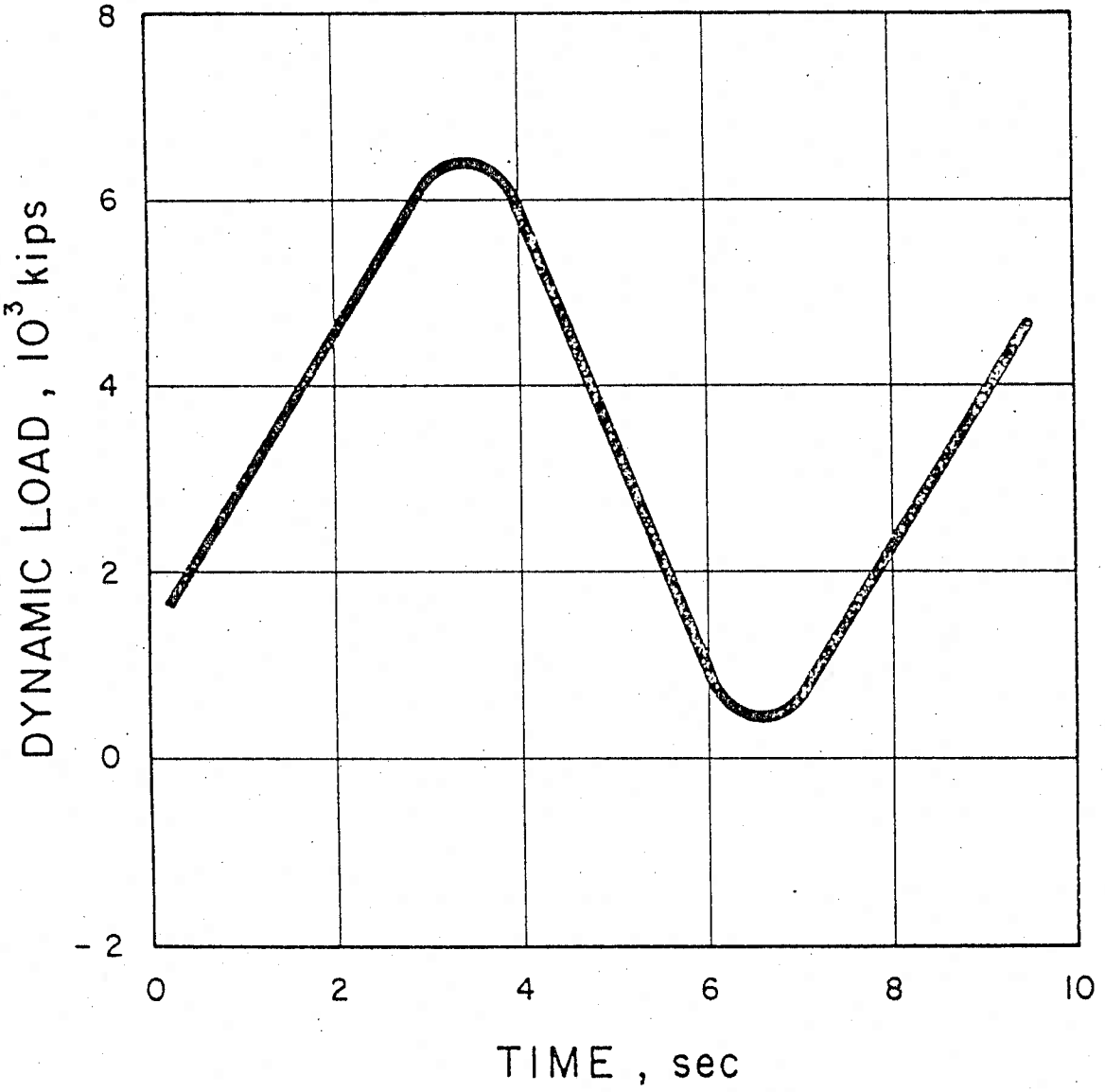

FIG. 6 TIME HISTORY OF DESIGN DYNAMIC LOADING ON EXAMPLE PLATFORM IN 1000 FEET OF WATER, GULF OF MEXICO

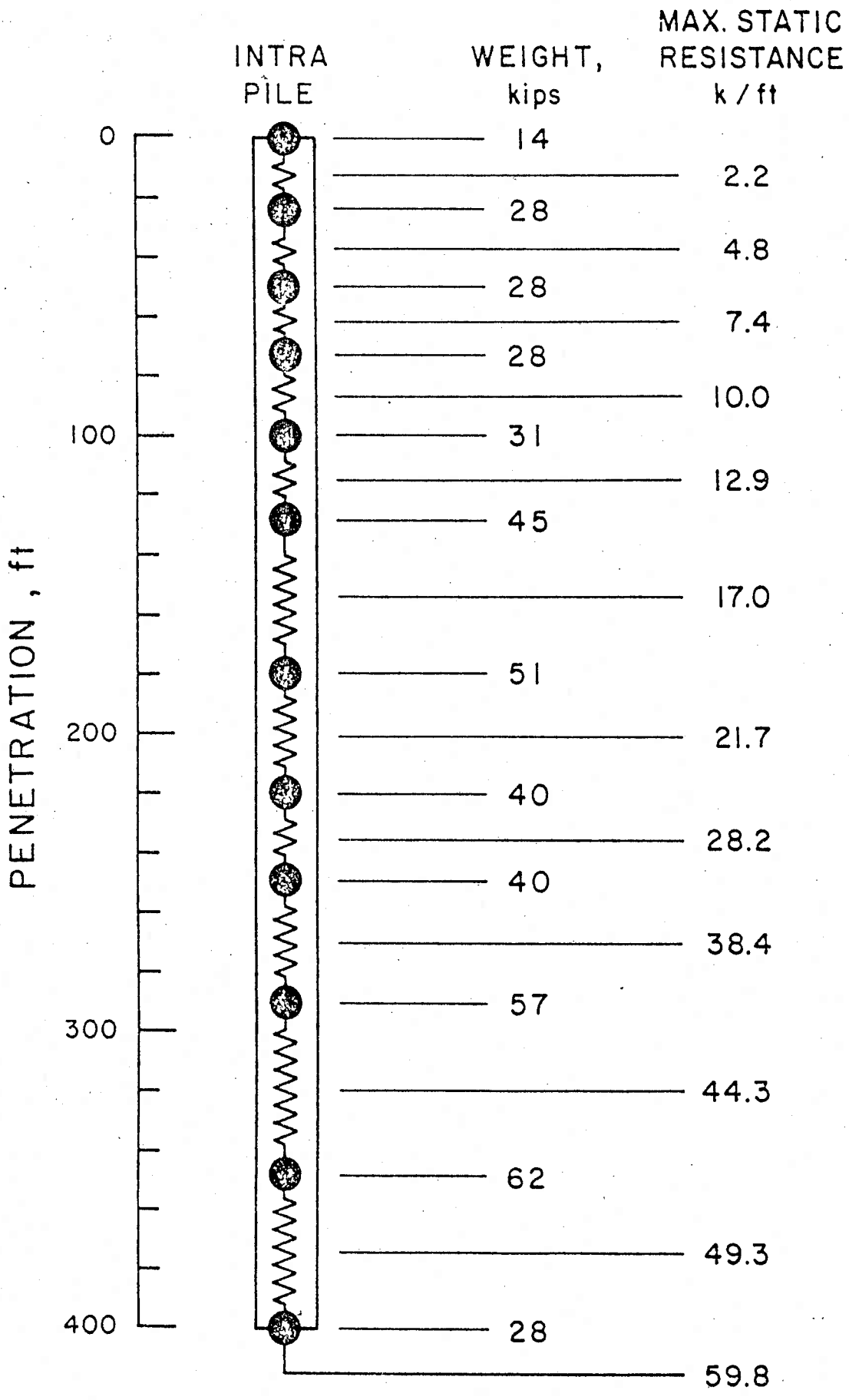

FIG. 7 INTRA MODEL OF 400 FOOT LONG PILE

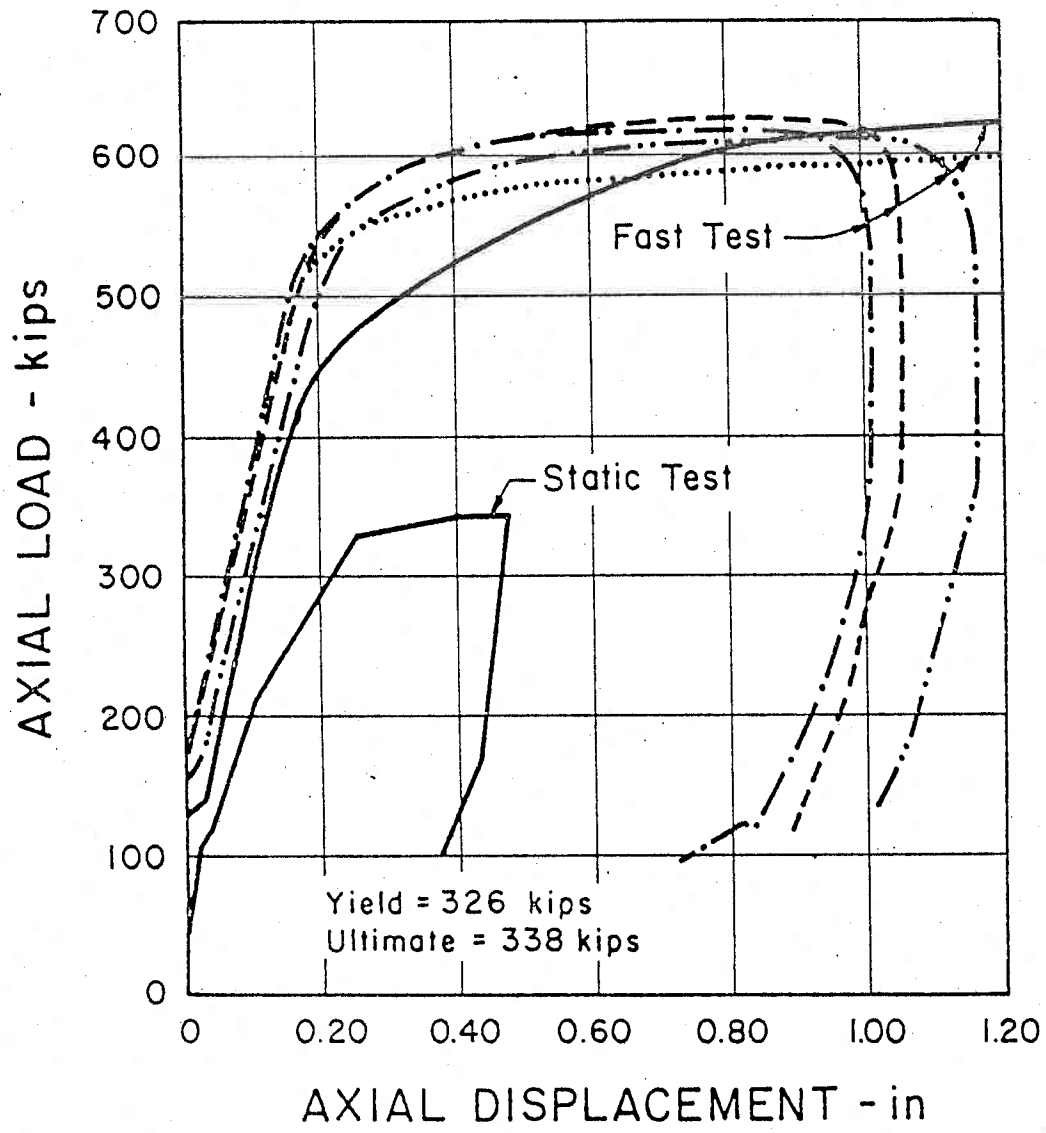

FIG. 8 TEST PILE MEASURED LOAD-DISPLACEMENT FOR STATIC AND DYNAMIC TESTS

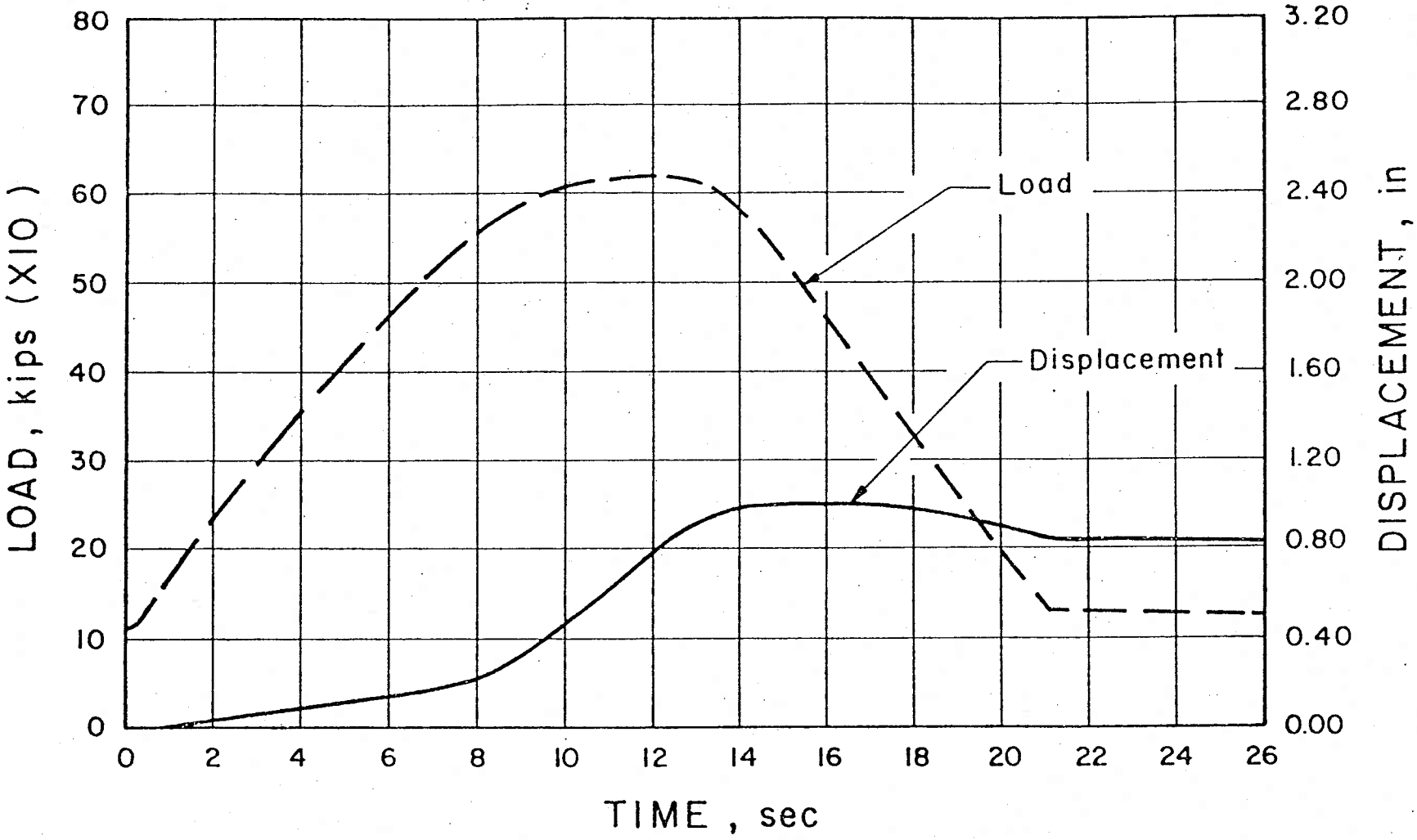

FIG. 9 TEST PILE MEASURED LOAD AND DISPLACEMENT TIME HISTORY FOR DYNAMIC TEST

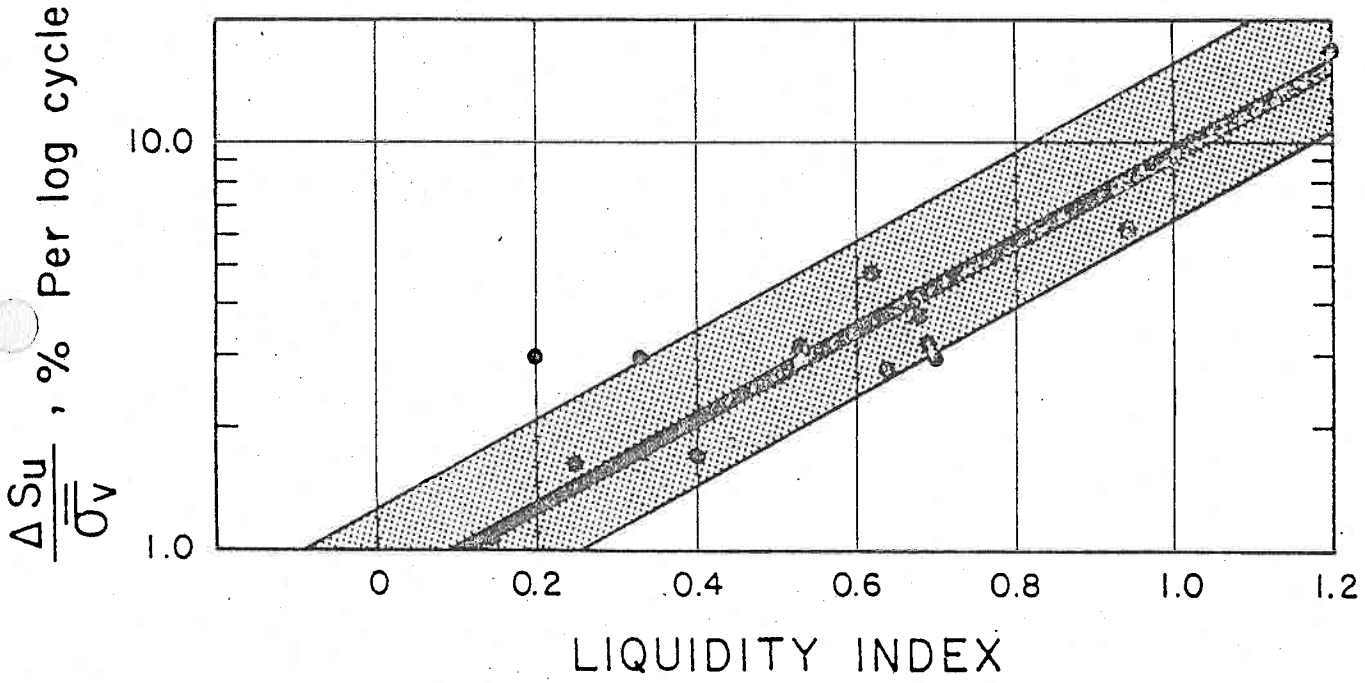

FIG. 10 INCREASE IN UNDRAINED SOIL SHEAR STRENGTH WITH INCREASED STRAIN RATE FOR NORMALLY CONSOLIDATED CLAYS

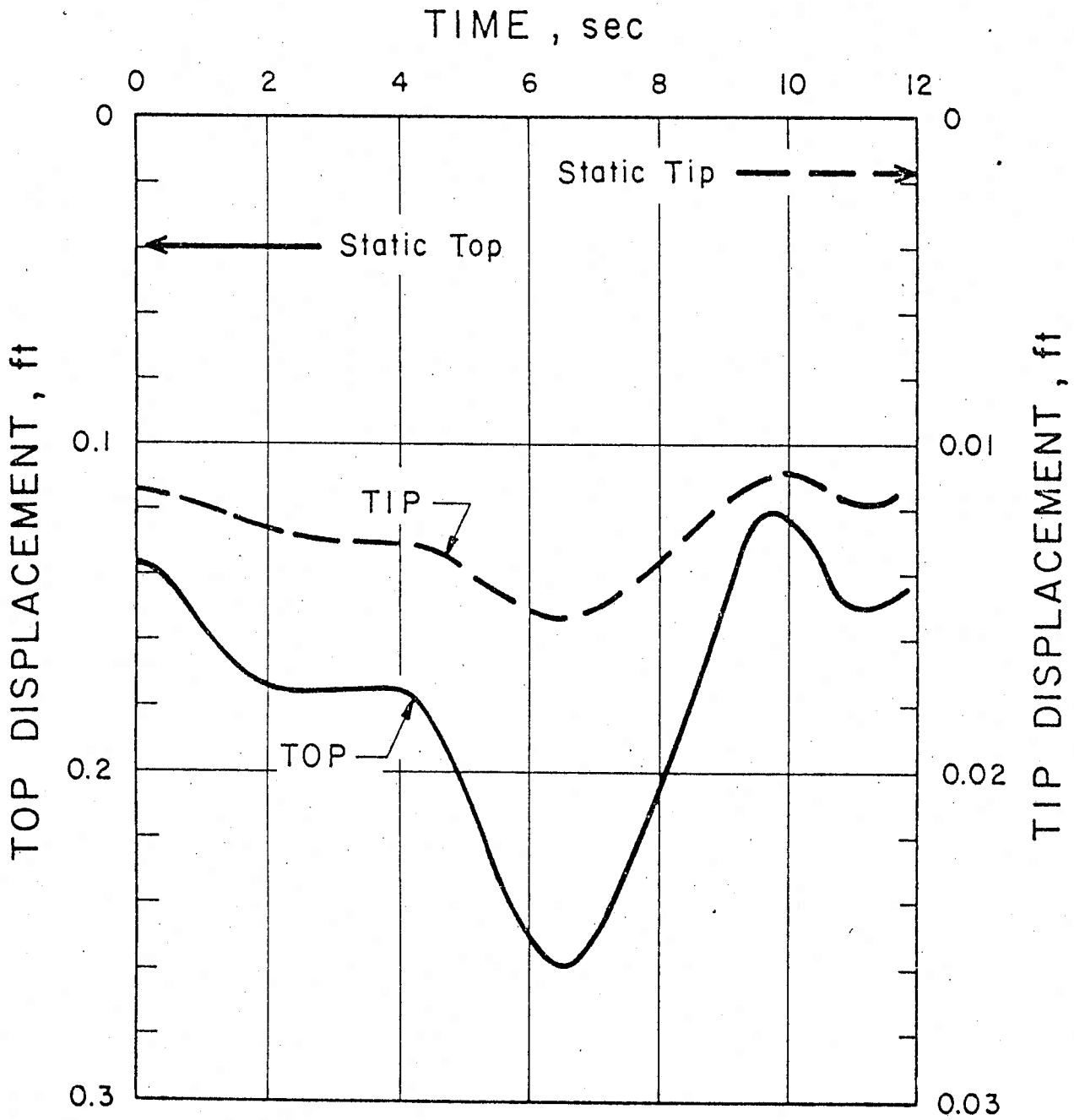

FIG. 11 COMPUTED TIME HISTORY OF DISPLACEMENT FOR PILE TOP AND TIP, 400 FOOT LONG PILE 72 INCHES IN DIAMETER

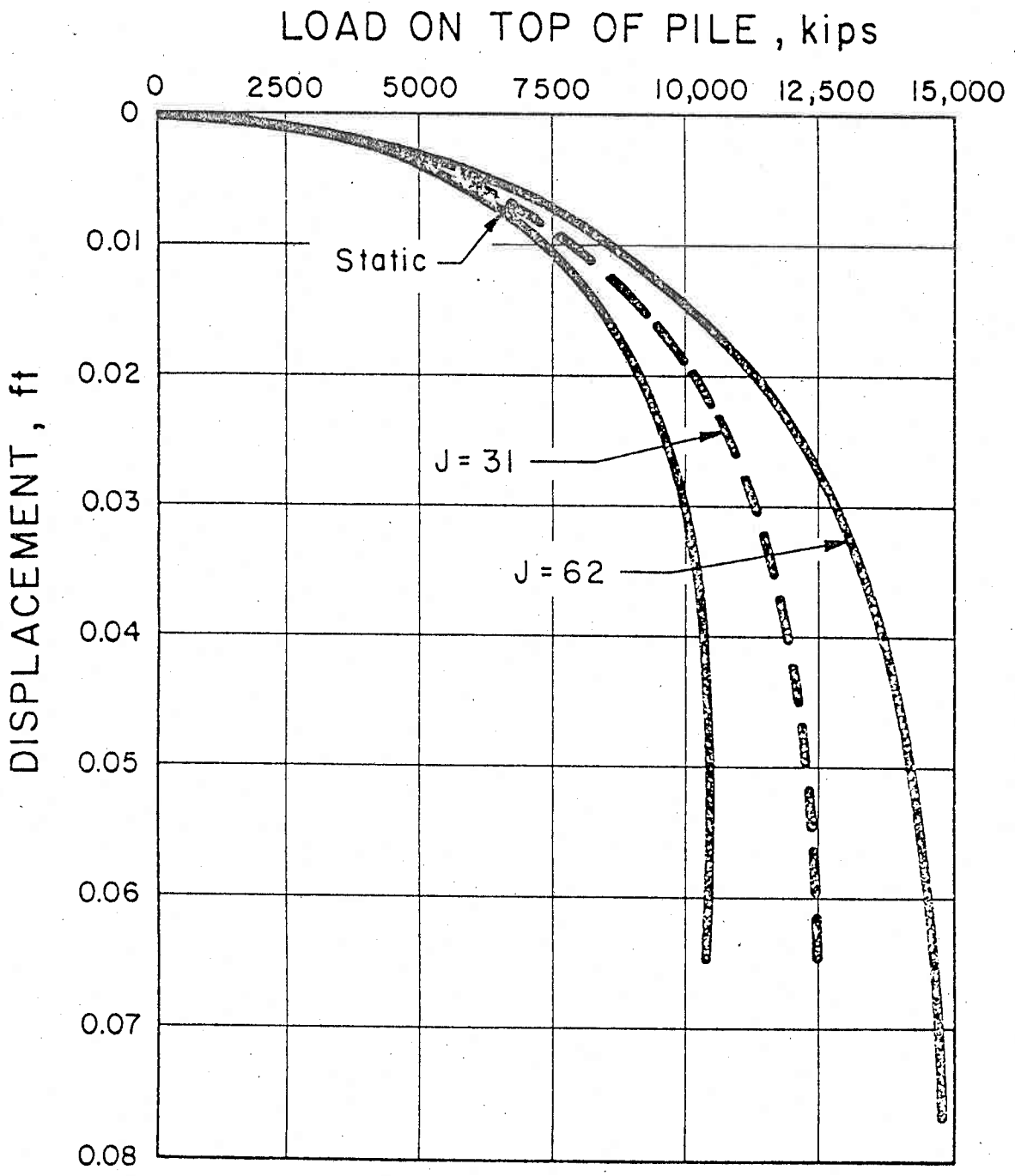

FIG. 12 DYNAMIC PEAK LOAD-DISPLACEMENT COMPARED WITH STATIC LOAD-DISPLACEMENT

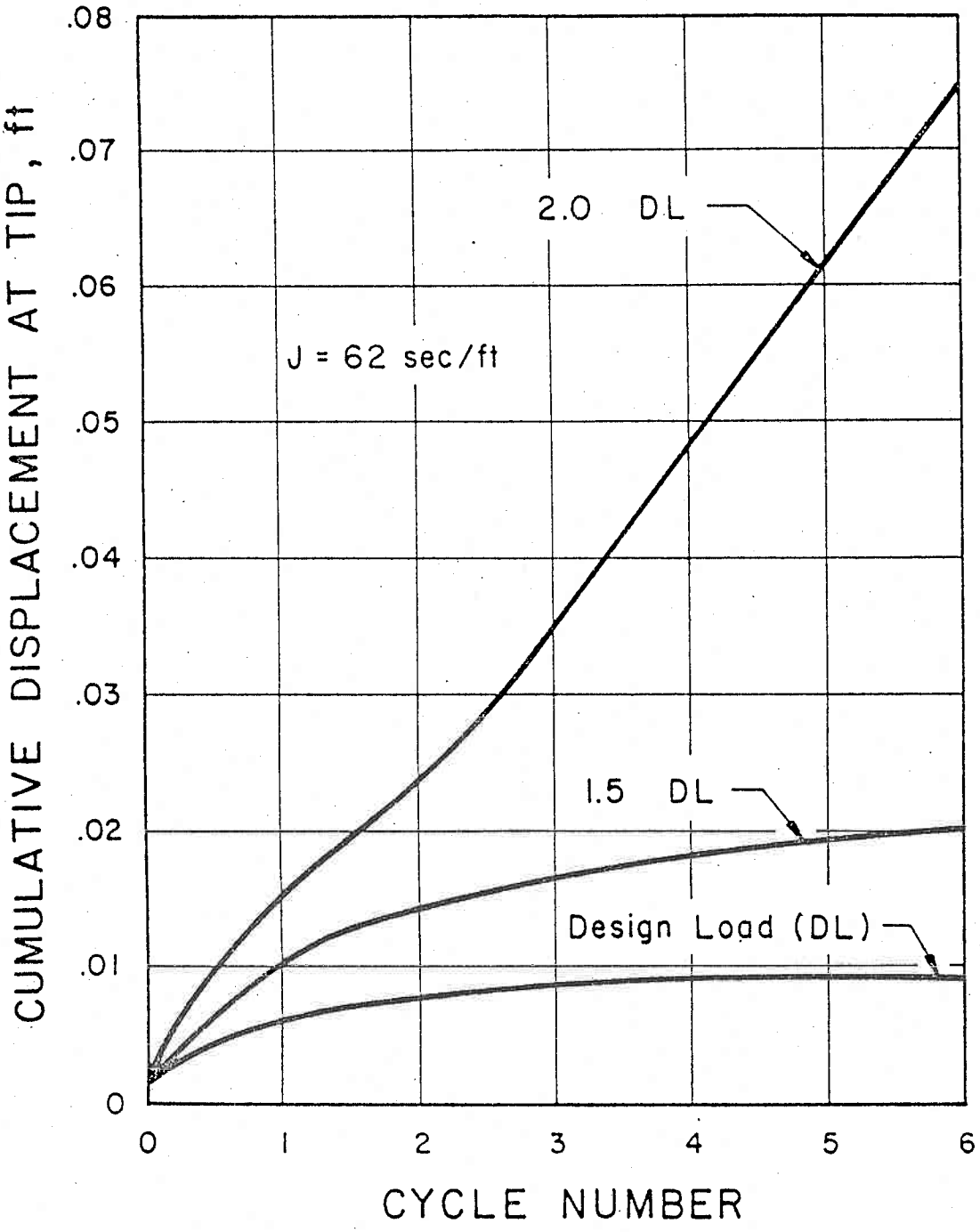

FIG. 13 NUMBERS OF CYCLES AND INCREASING MAGNITUDE OF DYNAMIC LOADING